JCI insight

RESEARCH ARTICLE

Activation of the calcium-sensing receptor attenuates TRPV6-dependent intestinal calcium absorption

Justin J. Lee,[1,2] Xiong Liu,[1] Debbie O'Neill,[1] Megan R. Beggs,[1,2] Petra Weissgerber,[3] Veit Flockerzi,[3] Xing-Zhen Chen,[1] Henrik Dimke,[4,5] and R. Todd Alexander[1,2,6]

[1]Department of Physiology, University of Alberta, Edmonton, Alberta, Canada. [2]The Women's and Children's Health Research Institute, Edmonton, Alberta, Canada. [3]Experimentelle und Klinische Pharmakologie und Toxikologie, Saarland University, Hamburg, Germany. [4]Department of Cardiovascular and Renal Research, Institute of Molecular Medicine, University of Southern Denmark, Odense, Denmark. [5]Department of Nephrology, Odense University Hospital, Odense, Denmark. [6]Department of Pediatrics, University of Alberta, Edmonton, Alberta, Canada.

Plasma calcium (Ca^{2+}) is maintained by amending the release of parathyroid hormone and through direct effects of the Ca^{2+}-sensing receptor (CaSR) in the renal tubule. Combined, these mechanisms alter intestinal Ca^{2+} absorption by modulating 1,25-dihydroxyvitamin D_3 production, bone resorption, and renal Ca^{2+} excretion. The CaSR is a therapeutic target in the treatment of secondary hyperparathyroidism and hypocalcemia, a common complication of calcimimetic therapy. The CaSR is also expressed in intestinal epithelium; however, a direct role in regulating local intestinal Ca^{2+} absorption is unknown. Chronic CaSR activation decreased expression of genes involved in Ca^{2+} absorption. In Ussing chambers, increasing extracellular Ca^{2+} or basolateral application of the calcimimetic cinacalcet decreased net Ca^{2+} absorption across intestinal preparations acutely. Conversely, Ca^{2+} absorption increased with decreasing extracellular Ca^{2+} concentration. These responses were absent in mice expressing a nonfunctional TRPV6, TRPV6^{D541A}. Cinacalcet also attenuated Ca^{2+} fluxes through TRPV6 in *Xenopus* oocytes when coexpressed with the CaSR. Moreover, the phospholipase C inhibitor U73122 prevented cinacalcet-mediated inhibition of Ca^{2+} flux. These results reveal a regulatory pathway whereby activation of the CaSR in the basolateral membrane of the intestine directly attenuates local Ca^{2+} absorption via TRPV6 to prevent hypercalcemia and help explain how calcimimetics induce hypocalcemia.

Introduction

Calcium (Ca^{2+}) homeostasis is vital to many physiological functions and is thus tightly regulated by altering Ca^{2+} transport across intestine, kidneys, and bone. It has been appreciated for some time that endocrine hormones, including parathyroid hormone (PTH) and 1,25-dihydroxyvitamin D_3 (1,25-$[OH]_2$ D_3), alter Ca^{2+} transport across the intestine and kidneys or aid mobilization from bone (1–4). However, more recently, the homeostatic mechanisms permitting direct sensing of extracellular Ca^{2+} by the nephron or bone and subsequently altering tubular Ca^{2+} reabsorption or bone remodeling were delineated (5, 6). This direct sensing of extracellular Ca^{2+} occurs, at least in part, by the 7-transmembrane G protein–coupled Ca^{2+} sensing receptor (CaSR) (7).

PTH release from the parathyroid gland increases plasma Ca^{2+} levels through direct effects on the nephron and bone and indirect effects on the intestine via stimulation of renal CYP27B1 activity, which catalyzes the synthesis of 1,25-$[OH]_2$ D_3 (8–11). PTH secretion is regulated by the CaSR, where increased extracellular Ca^{2+} activates the receptor, inhibiting release of PTH (12–14) and hence formation of 1,25-$[OH]_2$ D_3. In the thick ascending limb (TAL), blood Ca^{2+} concentration is also sensed by the basolateral CaSR, which directly signals to decrease Ca^{2+} reabsorption in that nephron segment (15–18). Conversely, PTH stimulates Ca^{2+} absorption from the TAL (18, 19) and transcellular Ca^{2+} reabsorption from the distal convoluted tubule (DCT) and connecting tubule (CNT) (20–22). These studies highlight how the renal tubule both responds to endocrine regulation, and directly senses extracellular Ca^{2+}, to amend Ca^{2+} reabsorption, thereby preventing hypercalcemia.

The duodenum, cecum, and proximal colon are sites of significant intestinal transcellular Ca^{2+} absorption (23, 24). Transcellular Ca^{2+} transport is a unidirectional, ATP-driven process mediated, at least in part, by the

Conflict of interest: RTA has consulted for Ardylex Inc. and Advicenne Inc.

Submitted: February 7, 2019
Accepted: April 17, 2019
Published: June 6, 2019.

Reference information: *JCI Insight*. 2019;4(11):e128013. https://doi.org/10.1172/jci.insight.128013.

apically expressed channel TRPV6, the intracellular Ca^{2+}-buffering protein calbindin-D_{9k} (CABP9K), and the basolateral Ca^{2+}-extruding proteins plasma membrane Ca^{2+} ATPase 1b (PMCA1b) and Na^+/Ca^{2+}-exchanger (NCX1) (23). Hypocalcemia leads to increased PTH secretion, which stimulates the production of 1,25-$[OH]_2$ D_3 and thus increases intestinal Ca^{2+} transport (8–11). 1,25-$[OH]_2$ D_3 increases intestinal Ca^{2+} absorption by increasing the expression of TRPV6, a phenomenon that correlates with intestinal Ca^{2+} absorption (24–26). The resulting increased Ca^{2+} influx in turn enhances the expression of CABP9K (27–29). Conversely, hypercalcemia inhibits PTH release and consequently reduces intestinal Ca^{2+} uptake, by limiting active 1,25-$[OH]_2$ D_3 synthesis. However, this latter regulatory mechanism would be rather slow with respect to attenuating hypercalcemia.

The CaSR is expressed throughout the intestine (30–32), where it regulates fluid, sodium, and chloride secretion (32–34). However, a direct role in Ca^{2+} homeostasis has not been reported (7, 33). We hypothesized that the intestinal CaSR has a functional role in maintaining Ca^{2+} homeostasis, where it detects extracellular Ca^{2+} levels and directly alters transcellular Ca^{2+} absorption across the sensing intestinal epithelium in response. To test our hypothesis, we first examined the expression of transcellular Ca^{2+}-transporting proteins following chronic CaSR activation and found decreased expression of genes known to facilitate transcellular Ca^{2+} absorption across the intestine. We further observed that acute pharmacological or physiological activation of a basolateral CaSR in intestinal epithelium ex vivo attenuated transcellular Ca^{2+} absorption. Moreover, this attenuation was absent in transgenic mice expressing functionally inactive TRPV6 Ca^{2+} channels. Together, our results demonstrate that basolateral activation of an intestinal CaSR directly inhibits local Ca^{2+} absorption from that intestinal segment via TRPV6.

Results

Activation of an intestinal CaSR decreases expression of genes involved in transcellular Ca^{2+} absorption. The expression of genes mediating transcellular Ca^{2+} absorption was measured on intestinal tissue from FVB/N mice fed a low (0.01%), normal (0.6%), or high (2%) Ca^{2+} diet for 21 days. *Trpv6* mRNA expression was increased in mice fed a low-Ca^{2+} diet, with the greatest, greater than 30-fold increase, observed in the proximal colon (Figure 1A). A high-Ca^{2+} diet suppressed *Trpv6* expression in the duodenum, cecum, and proximal colon, perhaps because of low 1,25-$[OH]_2$ D_3, although a direct inhibitory effect of plasma Ca^{2+} cannot be excluded. The same relationship, between increased dietary Ca^{2+} content and reduced gene expression, was observed for *S100g*, which encodes the intracellular Ca^{2+}-buffering and -shuttling protein CABP9K. The mRNA expression of the basolateral Ca^{2+} efflux transporters NCX1 (*Slc8a1*) and PMCA1b (*Atp2b1*) were unaltered in all tissues under different dietary calcium–containing conditions (Figure 1, A–C).

The serum Ca^{2+} of mice fed altered-Ca^{2+} diets was not different from that of mice fed a normal-Ca^{2+} diet (15). This was likely the result of altered 1,25-$[OH]_2$ D_3 production induced by varying Ca^{2+}-containing diets (28, 35, 36). To assess the effect of 1,25-$[OH]_2$ D_3 on the intestinal expression of genes mediating transcellular Ca^{2+} transport, mice were directly administered (via intraperitoneal injection) 1,25-$[OH]_2$ D_3 (500 pg/g body weight) for 5 days and the studies were repeated (15). This increased expression of *Trpv6* and *S100g* (Figure 1, E and F). These data are consistent with the observation that 1,25-$[OH]_2$ D_3 enhances intestinal Ca^{2+} absorption via increased expression of TRPV6 (37). Interestingly, the increase was less pronounced than what was observed on a low-Ca^{2+} diet, even though serum 1,25-$[OH]_2$ D_3 levels were increased to a greater extent (15). However, the 1,25-$[OH]_2$ D_3–injected mice were markedly hypercalcemic, potentially attenuating the increased expression induced by 1,25-$[OH]_2$ D_3 (15).

To examine the effect of CaSR activation on *Trpv6*, *S100g*, *Slc8a1*, and *Atp2b1* expression, we administered the calcimimetic cinacalcet (1 mg/g body weight) for 5 days. *Trpv6* expression was reduced in cinacalcet-treated mice (Figure 1, G–I). Importantly, PTH and serum Ca^{2+} were substantially lower in cinacalcet-treated mice; however, 1,25-$[OH]_2$ D_3 levels were not altered by cinacalcet (15). In addition, expression of *S100g* and *Atp2b1* was reduced in the cecum of cinacalcet-treated mice (Figure 1H), and all genes involved in transcellular Ca^{2+} absorption were decreased in the proximal colon of cinacalcet-treated animals (Figure 1I). Together, these results are consistent with direct Ca^{2+} sensing by the intestine decreasing transcellular Ca^{2+} absorption via decreasing the expression of genes mediating transcellular Ca^{2+} absorption.

Extracellular Ca^{2+} inhibits transcellular Ca^{2+} absorption in the proximal colon. Next, we sought to determine whether a direct Ca^{2+}-sensing mechanism regulates intestinal Ca^{2+} absorption independent of calciotropic hormones. To do so, we measured net Ca^{2+} flux across the proximal colon ex vivo in Ussing chambers (i.e., net Ca^{2+} flux = unidirectional apical-to-basolateral Ca^{2+} flux – unidirectional basolateral-to-apical Ca^{2+} flux from the same segment and animal). We chose to study this segment initially as it had the largest changes

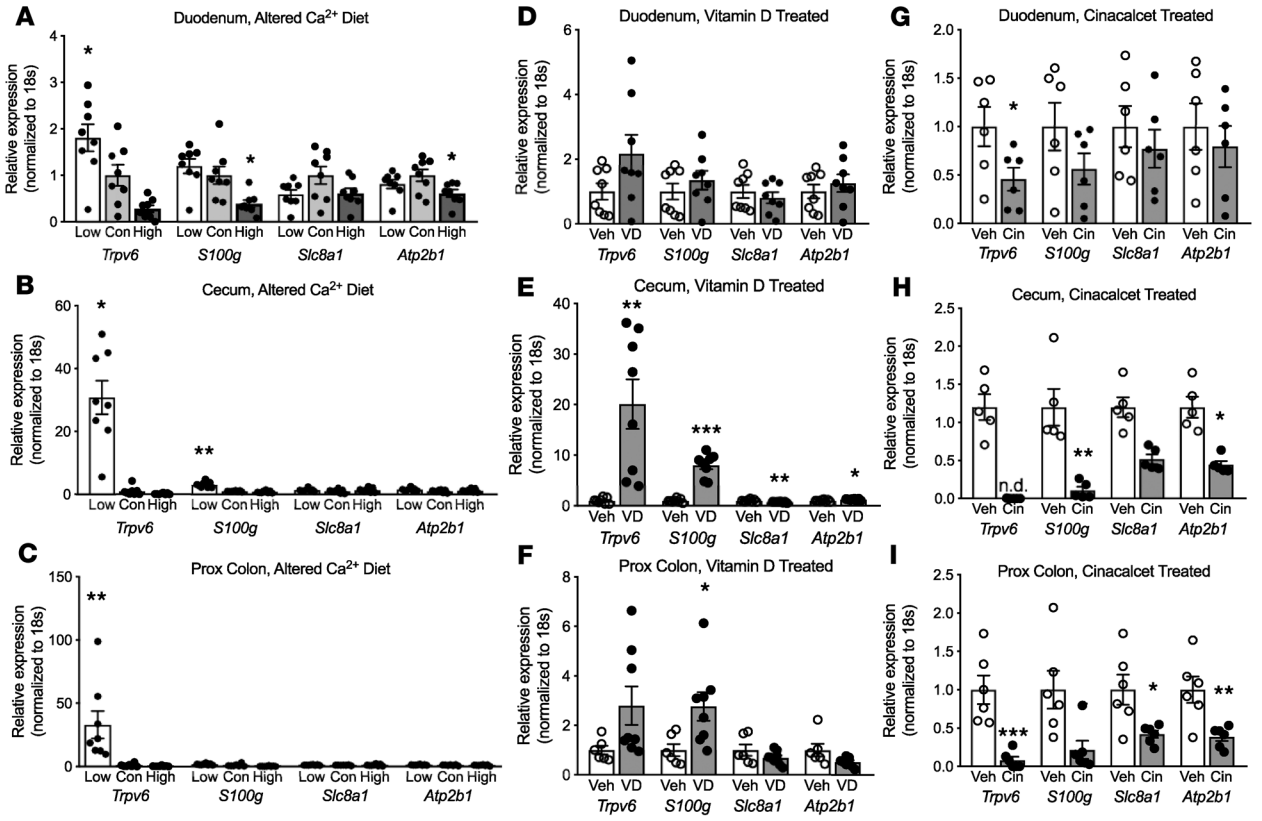

Figure 1. Relative intestinal mRNA expression of transcellular Ca^{2+} transport mediators under altered extracellular Ca^{2+} conditions. (**A**–**C**) Relative mRNA expression of transcellular Ca^{2+} transport mediators TRPV6 (*Trpv6*), CABP9K (*S100g*), NCX1 (*Slc8a1*), or PMCA1b (*Atp2b1*), normalized to 18S rRNA expression in mice on high-, normal- (Con), or low-Ca^{2+} diet for 21 days (n = 7 for each diet). (**D**–**F**) Relative mRNA expression in animals treated with 1,25-$[OH]_2$ D_3 (VD) or vehicle (Veh) (n = 8 for each). (**G**–**I**) Relative mRNA expression in animals treated with cinacalcet (Cin) or control (Veh) diet (n = 8 for each). All data are presented as the mean ± SEM, normalized to the mice on the normal/control diet. Asterisks indicate a statistically significant difference from the normal/control mice by 1-way ANOVA (all genes in **A** and *Slc8a1* and *Atp2b1* in **B** and **C**), Brown-Forsythe test (*S100g* in **B**), Kruskal-Wallis test (*Trpv6* in **B** and **C**), or Student's unpaired t tests (**D**–**I**); $^*P < 0.05$, $^{**}P < 0.01$, $^{***}P < 0.001$.

in expression (Figure 1), in addition to significant 1,25-$[OH]_2$ D_3–mediated regulation of transcellular Ca^{2+} absorption, as well as greater sojourn time and thus Ca^{2+} availability (29, 38, 39). Importantly, measurements of Ca^{2+} flux made in Ussing chambers enabled us to avoid the confounding effects of calciotropic hormones. The buffer bathing the tissue contained equal concentrations of Ca^{2+}, and the transepithelial voltage was clamped to 0 mV. This eliminated a net driving force for paracellular Ca^{2+} movement, enabling us to attribute net flux to movement through the transcellular Ca^{2+} transport pathway. The net Ca^{2+} flux obtained under condition A (control) was compared with the one obtained under condition B (i.e., bilateral application of cinacalcet, Figure 2). Figure 3A displays a typical short-circuit current trace recorded from a single channel. Bilateral cinacalcet administration significantly reduced net Ca^{2+} absorption (Figure 3B), consistent with the proximal colon sensing increased extracellular Ca^{2+} and attenuating Ca^{2+} absorption in response.

To implicate physiological changes in extracellular Ca^{2+} regulating transcellular Ca^{2+} absorption, we again examined net Ca^{2+} flux across proximal colon ex vivo in Ussing chambers before and after changing the Ca^{2+} concentration in the buffers simultaneously under voltage clamp conditions (i.e., buffers in both chambers were exchanged from bilaterally containing solutions with high Ca^{2+} (2.5 mM) to solutions with low Ca^{2+} (0.5 mM) to eliminate a transepithelial electrochemical gradient for calcium under both conditions). When the extracellular Ca^{2+} concentration was decreased, net Ca^{2+} flux increased, and conversely, when the extracellular Ca^{2+} concentration was increased, net Ca^{2+} flux decreased (Figure 3C). These results further support the idea that the proximal colon directly senses extracellular Ca^{2+} and acutely alters transcellular Ca^{2+} absorption to maintain plasma Ca^{2+} within physiological limits.

Increased basolateral extracellular Ca^{2+} attenuates transcellular Ca^{2+} absorption. The CaSR is expressed throughout rodent and human intestine (32, 40–42), including in both the apical and basolateral mem-

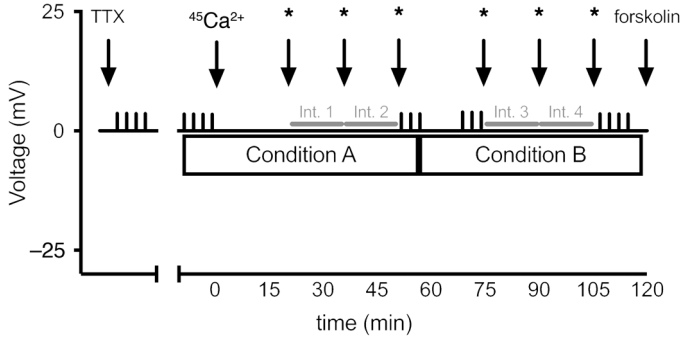

Figure 2. Protocol used to measure unidirectional Ca^{2+} fluxes across intestinal preparations. The transepithelial voltage across tissue preparations (*y* axis) was clamped to 0 mV for the duration of the experiment (*x* axis). The voltage spikes along the *x* axis correspond to 2-mV pulses applied and used to determine the transepithelial resistance (TER). We added 0.1 μM tetrodotoxin (TTX) basolaterally first and allowed the resulting short-circuit current to stabilize. At time 0, the solutions were exchanged for fresh ones with 1 side spiked with $^{45}Ca^{2+}$. Asterisks indicate the time points when samples were taken for radioactivity measurements. Two gray horizontal lines represent 15-minute time intervals, where unidirectional $^{45}Ca^{2+}$ flux was calculated for each condition. We added 10 μM forskolin at the end of the experiment to confirm tissue viability.

branes of proximal colonocytes (30–32). We confirmed intestinal CaSR expression by measuring mRNA via quantitative real-time PCR (Figure 4A). Next, to determine whether apical and/or basolateral Ca^{2+} sensing mediates decreased transcellular Ca^{2+} absorption, we measured net Ca^{2+} flux as above but applied cinacalcet to either the basolateral or the apical hemichamber. Apical application of cinacalcet did not alter net Ca^{2+} flux (Figure 4B). In contrast, basolateral treatment significantly decreased net Ca^{2+} flux (Figure 4C). Moreover, basolateral application of cinacalcet attenuated net Ca^{2+} flux across the duodenum and the cecum, other sites of transcellular Ca^{2+} absorption (Supplemental Figure 1; supplemental material available online with this article; https://doi.org/10.1172/jci.insight.128013DS1). These data are consistent with basolateral CaSR signaling decreasing transcellular intestinal Ca^{2+} absorption.

TRPV6-mediated Ca^{2+} absorption is attenuated by CaSR activation. To identify the channel regulating transcellular Ca^{2+} flux in response to increased basolateral extracellular Ca^{2+}, we repeated the Ca^{2+} flux studies on wild-type ($TRPV6^{WT/WT}$) and $TRPV6^{D541A/D541A}$-knockin mice. These animals express TRPV6 with mutation D541A in the pore loop, rendering it nonfunctional (43). Interestingly, $TRPV6^{WT/WT}$ mice had significantly greater net Ca^{2+} flux across the proximal colon under control conditions (condition A), compared with $TRPV6^{D541A/D541A}$ mice (Figure 5A). Moreover, $TRPV6^{WT/WT}$ mice reduced net Ca^{2+} flux in response to basolateral cinacalcet treatment, in contrast with $TRPV6^{D541A/D541A}$ mice, where net Ca^{2+} flux was unchanged (Figure 5A).

Because $TRPV6^{D541/D541A}$ mice do not display net Ca^{2+} flux at baseline, we sought to stimulate net Ca^{2+} flux by exposing proximal colon to high–extracellular Ca^{2+} buffer and then lowering extracellular Ca^{2+}. Again, $TRPV6^{WT/WT}$ mice had significantly greater net Ca^{2+} flux at baseline compared with the $TRPV6^{D541A/D541A}$ mice (Figure 5B). As observed for wild-type FVB/N mice, when proximal colon from $TRPV6^{WT/WT}$ mice was switched from a high- to a low-Ca^{2+} buffer, net Ca^{2+} flux increased. This was in contrast with $TRPV6^{D541A/D541A}$ mice, where no change in net Ca^{2+} flux was observed. These results implicate TRPV6 in mediating transcellular Ca^{2+} absorption across the proximal colon in response to changes in basolateral extracellular Ca^{2+}.

CaSR expression is sufficient for TRPV6 to respond to extracellular Ca^{2+}. To understand how the CaSR may confer acute inhibition of Ca^{2+} flux through TRPV6, we sought to reconstitute the system in vitro. To this end, we expressed human TRPV6 and the CaSR in *Xenopus* oocytes and measured the Ca^{2+} current (I_{Ca}). We chose this system to study the effect of CaSR activation on TRPV6 activity because it lacks endogenous G protein–coupled receptors that are often present in mammalian cell culture models. Oocytes expressing TRPV6 alone failed to decrease I_{Ca} after incubation with cinacalcet (Supplemental Figure 2 and ref. 44). In contrast, oocytes coexpressing the CaSR and TRPV6 displayed a significant reduction in I_{Ca} after cinacalcet treatment (Figure 6A). These results are consistent with our ex vivo observation that CaSR activation inhibits Ca^{2+} flux through TRPV6.

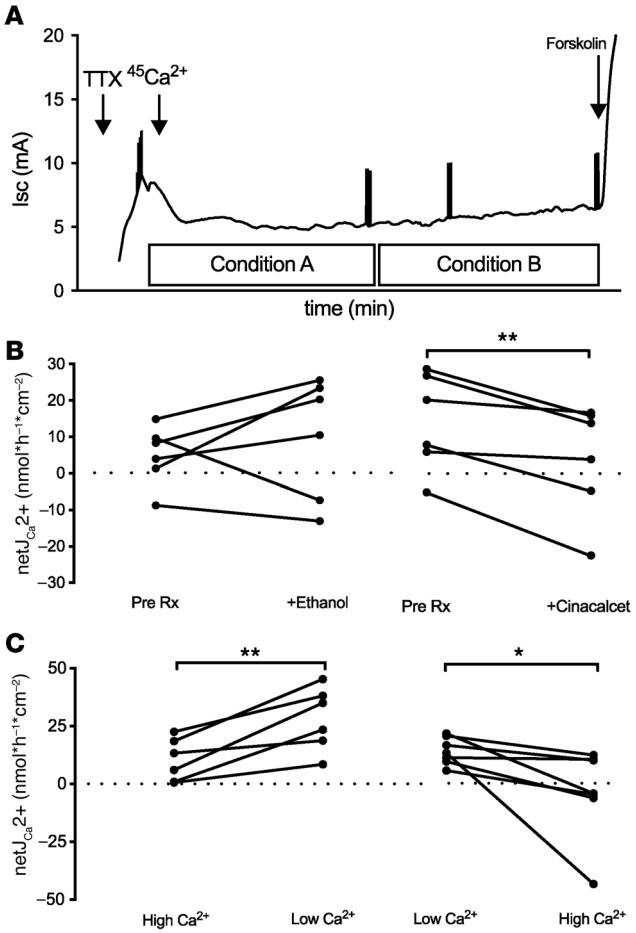

Figure 3. The effect of altering extracellular Ca^{2+} on Ca^{2+} fluxes across mouse proximal colon. (**A**) An example of the short-circuit current (I_{SC}) recorded throughout protocol 1. TTX was added and I_{SC} allowed to stabilize. The I_{SC} spikes occurred in response to 2-mV pulses. At the second arrow, solutions were exchanged, with 1 side only containing $^{45}Ca^{2+}$. The tissue was deemed viable if the I_{SC} increased more than 3 times with forskolin administration at the end of the experiment. (**B**) Changes in the net Ca^{2+} flux (net J_{Ca}^{2+}) between condition A, pretreatment (Pre Rx), and condition B, vehicle (ethanol) or 10 μM cinacalcet (n = 6 each treatment). (**C**) The change in net J_{Ca}^{2+} between condition A, high Ca^{2+} (2.5 mM), and condition B, low-Ca^{2+} (0.5 mM), or the converse (n = 6 each). Raw values are presented; asterisks indicate a statistical difference between the conditions (Student's paired t tests; $^{*}P < 0.05$, and $^{**}P < 0.01$).

PLC regulates *Trpv6* in vitro (45–49). We therefore measured normalized I_{Ca} in TRPV6- and CaSR-expressing oocytes in the presence of U73122 (5 μM), a PLC inhibitor, or in the presence of U73122 and cinacalcet. The PLC inhibitor increased I_{Ca} even in the absence of the CaSR (Supplemental Figure 2). Further, PLC inhibition increased I_{Ca} in the absence and presence of cinacalcet, implicating PLC inhibition in the CaSR-mediated decrease in TRPV6 activity (Figure 6A and Supplemental Figure 3). We next examined the effects of cinacalcet and U73122 on total and surface expression of TRPV6 and the CaSR in *Xenopus* oocytes and found that membrane expression was not altered by either drug (Figure 6, B and C; see complete unedited blots in the supplemental material). Together, these data implicate the PLC pathway in the inhibition of TRPV6 channel activity by the CaSR.

CaSR activation inhibits transcellular Ca^{2+} absorption via PLC activation. Finally, the involvement of PLC in CaSR-mediated regulation of TRPV6 was investigated in the proximal colon ex vivo. To this end, we again used the PLC inhibitor U73122 in combination with cinacalcet in Ussing chambers. For these experiments, we had a similar condition A (control condition), but for condition B, we administered either cinacalcet plus vehicle (DMSO) or cinacalcet plus U73122. The cinacalcet/vehicle–treated group displayed a significant decrease in net Ca^{2+} flux (Figure 6D). However, co-incubation with the PLC inhibitor prevented the inhibitory effect of cinacalcet (Figure 6D). These data are in agreement

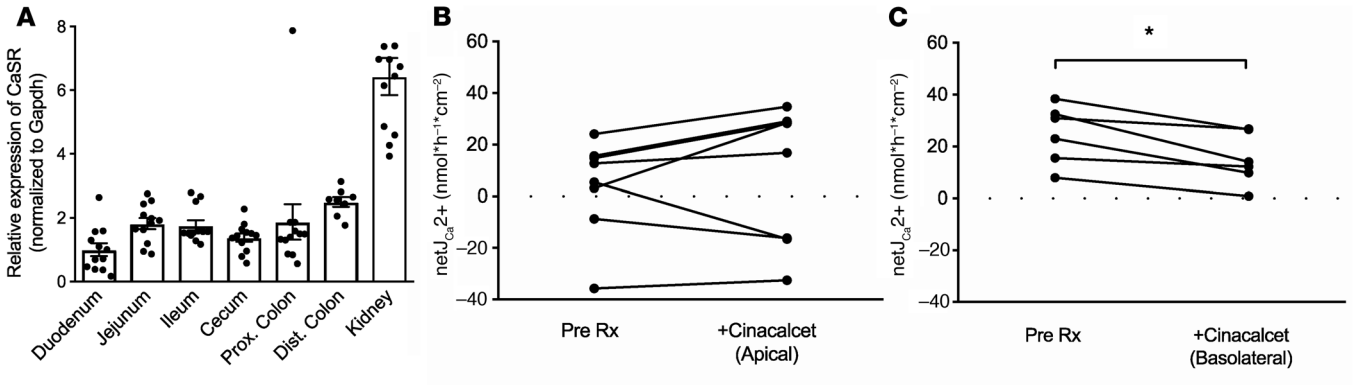

Figure 4. Expression of the CaSR and effect of apical or basolateral CaSR activation. (**A**) Relative mRNA expression of the CaSR throughout mouse intestine (n = 12), normalized to duodenum. (**B** and **C**) Changes in the net J_{Ca}^{2+} in the proximal colon of wild-type mice between condition A, pretreatment, and condition B, apical or basolateral 10 μM cinacalcet application (n = 7 each application in **B**; n = 6 in **C**). Raw values are presented; asterisks indicate a statistical difference between the conditions (Student's paired t tests; $^*P < 0.05$).

with our in vitro data (Figure 6) and together imply that basolateral CaSR activation decreases transcellular Ca^{2+} transport through TRPV6 via a CaSR-induced activation of PLC in the proximal colon.

Discussion

The CaSR is expressed throughout the intestine; however, a direct role for the intestinal CaSR in maintaining Ca^{2+} homeostasis has not been described (7, 33). Alterations in plasma Ca^{2+} indirectly regulate plasma Ca^{2+} via altering PTH secretion and consequently 1,25-$[OH]_2$ D_3 production (37, 50, 51). In general, adjustment of intestinal Ca^{2+} absorption has been thought to occur by reducing circulating 1,25-$[OH]_2$ D_3, secondary to a decrease in PTH secretion induced by lower blood Ca^{2+} levels. However, such a mechanism would be slow to respond to acute elevations in serum Ca^{2+}. We therefore tested whether the intestine can directly adjust Ca^{2+} absorption in response to extracellular Ca^{2+}. Herein, we report that the intestine has a direct extracellular Ca^{2+}-sensing mechanism, which alters transcellular Ca^{2+} absorption through TRPV6. This is predominantly based on 3 observations: (a) both increased extracellular Ca^{2+} and a calcimimetic decreased transcellular Ca^{2+} absorption in Ussing chambers ex vivo; (b) this alteration in transcellular Ca^{2+} absorption is driven by TRPV6 because $TRPV6^{WT/WT}$, but not $TRPV6^{D541A/D541A}$ mice, alter transcellular Ca^{2+} flux in response to changes in extracellular Ca^{2+}; and (c) extracellular Ca^{2+} in the presence of the CaSR, but not in its absence, inhibits Ca^{2+}-mediated TRPV6 currents in oocytes, a process involving PLC in vitro and ex vivo. Taken together, these results reveal a mechanism in the bowel whereby alterations in plasma Ca^{2+} are detected by a basolateral CaSR, which amends Ca^{2+} absorption via a TRPV6 pathway to maintain Ca^{2+} homeostasis (Figure 7).

PTH increases production of 1,25-$[OH]_2$ D_3, which acts on the intestine to increase Ca^{2+} absorption (24–26). Consistent with this, our data show that mice fed a low Ca^{2+} diet had increased plasma 1,25-$[OH]_2$ D_3, but maintained normal plasma Ca^{2+} (15), and had increased expression of transcellular Ca^{2+} absorption mediators. In addition, direct administration of 1,25-$[OH]_2$ D_3 increased expression of intestinal transcellular Ca^{2+} absorption mediators. However, the degree of increased expression observed was less in the 1,25-$[OH]_2$ D_3–injected group than the mice on a low-Ca^{2+} diet. Interestingly, the mice administered 1,25-$[OH]_2$ D_3 also had increased plasma Ca^{2+}, which could have attenuated gene expression via a direct effect on the intestinal CaSR (15). Conversely, a high-Ca^{2+} diet decreased expression of these mediators of transcellular Ca^{2+} absorption. This may be due to decreased secretion of PTH and therefore decreased activation of 1,25-$[OH]_2$ D_3 (15). However, it might also be a result of chronic activation of the basolateral intestinal CaSR directly altering expression of transcellular Ca^{2+} absorption mediators. Consistent with this, administration of the calcimimetic cinacalcet suppressed plasma PTH levels and *Trpv6* and *S100g* expression, without altering plasma 1,25-$[OH]_2$ D_3 (15). Reduced circulating PTH could decrease 1,25-$[OH]_2$ D_3 levels and consequently reduce the expression of transcellular Ca^{2+} absorption mediators. However, cinacalcet-treated mice did not have reduced circulating 1,25-$[OH]_2$ D_3 (15). Thus, decreased *Trpv6* and *S100g* expression are not a result of PTH-dependent reduction in 1,25-$[OH]_2$ D_3 but instead are potentially due to a direct activation of an intestinal CaSR. Interestingly,

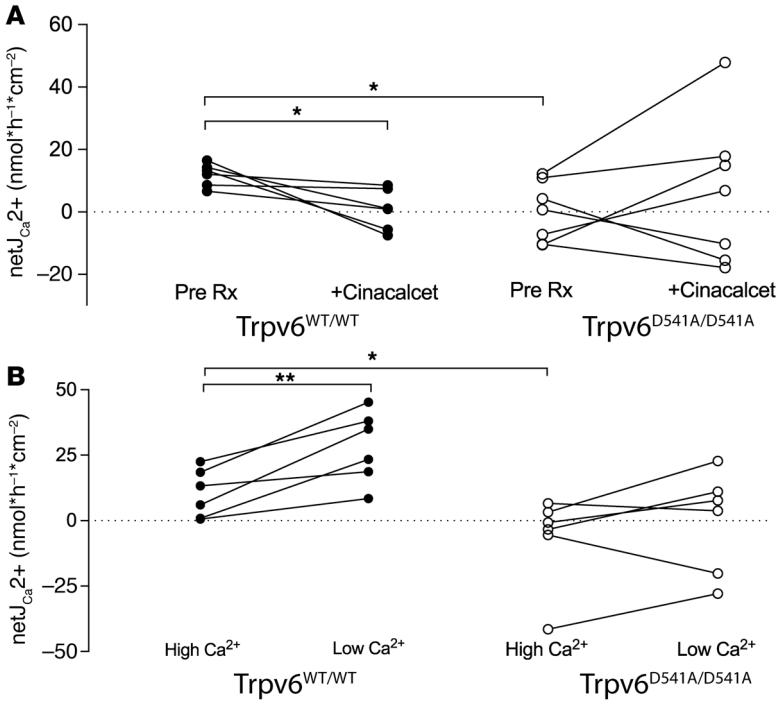

Figure 5. Effect of extracellular Ca^{2+} on Ca^{2+} fluxes across proximal colon from TRPV6$^{WT/WT}$ or TRPV6$^{D541A/D541A}$ mice. (**A**) Change in net J_{Ca}^{2+} between condition A, pretreatment, and condition B, basolateral 10 μM cinacalcet application (n = 6 each). (**B**) Change in net J_{Ca}^{2+} between condition A, high Ca^{2+} (2.5 mM), and condition B, low Ca^{2+} (0.5 mM) (n = 6 each). Raw values are presented; asterisks indicate a statistical difference between conditions (Student's paired t test for within genotype comparisons or unpaired t tests for between genotype comparison; *P < 0.05, and **P < 0.01).

cinacalcet appears to suppress *Trpv6* and *S100g* expression to a greater extent than a high-Ca^{2+} diet (Figure 1). This is likely due to greater activation of the CaSR by the calcimimetic than the high-Ca^{2+} diet as reflected in the greater suppression of PTH by this intervention (15). It is noteworthy that we and others observed CaSR expression along the intestine (31, 32). Together, the data are consistent with the bowel altering transcellular Ca^{2+} absorption via transcriptional downregulation directly in response to increased extracellular Ca^{2+}, independent of 1,25-$[OH]_2$ D_3.

The current model of transcellular Ca^{2+} absorption suggests a significant role for TRPV6 (28, 35, 52). TRPV6 is transcriptionally regulated by 1,25-$[OH]_2$ D_3 and estrogen (8–11, 36). Here, we report alterations in *Trpv6* expression in response to extracellular Ca^{2+}, in the absence of altered 1,25-$[OH]_2$ D_3, adding intestinal CaSR activation to the list of transcriptional regulators. It should be noted that because CABP9K expression is regulated by cytosolic Ca^{2+}, the corresponding changes in CABP9K expression observed likely reflect decreased Ca^{2+} absorption, and therefore, decreased cytosolic Ca^{2+}, rather than a direct transcriptional response to CaSR activation (35, 36).

Not only have we observed a chronic transcriptional effect of extracellular Ca^{2+} on TRPV6 expression, but we also identified an acute, direct regulatory role of extracellular Ca^{2+} on TRPV6 activity. Decreased net Ca^{2+} flux was observed across proximal colon of TRPV6$^{WT/WT}$ mice, but not TRPV6$^{D541A/D541A}$-mutant mice, following basolateral CaSR activation. Similarly, the increased net intestinal Ca^{2+} absorption observed in TRPV6$^{WT/WT}$ mice in response to lower extracellular Ca^{2+} was not observed in TRPV6$^{D541A/D541A}$ mice. These observations directly implicate TRPV6 in mediating altered transcellular Ca^{2+} absorption in response to CaSR activation. This was confirmed in vitro with *Xenopus* oocytes. CaSR activation in oocytes expressing TRPV6 and the CaSR decreased TRPV6-mediated Ca^{2+} currents. Previous work found evidence of CaSR-mediated alterations in paracellular Ca^{2+} permeability in colonic and renal epithelium (15, 34, 53). However, our experimental setup allowed us to eliminate the driving force for passive paracellular Ca^{2+} transport (i.e., a transepithelial electrochemical gradient). Thus, our results reflect changes in the net Ca^{2+} flux via an active transcellular pathway. Together, these data strongly support the presence of an acute regulatory effect of the CaSR in modifying cellular Ca^{2+} uptake, and thus transcellular Ca^{2+} absorption, via TRPV6.

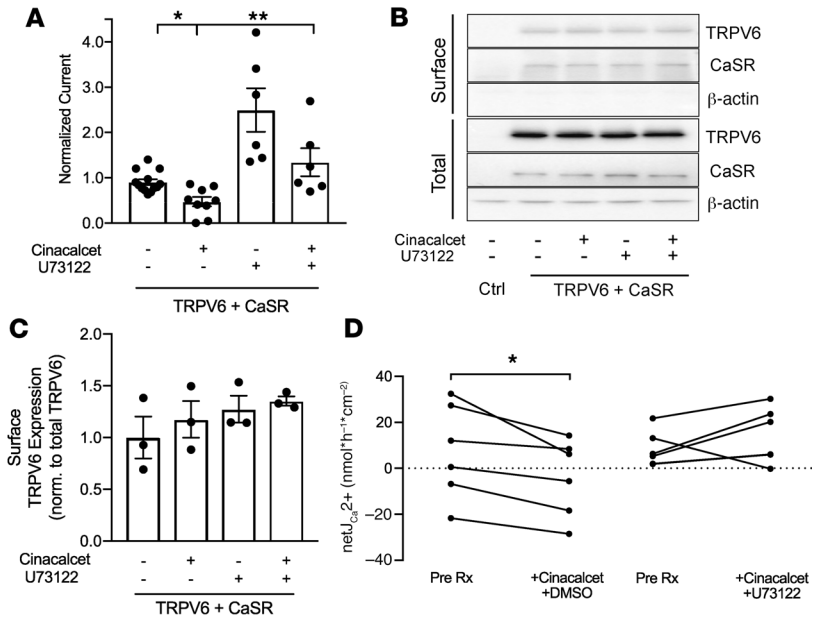

Figure 6. Effect of phospholipase C inhibition on CaSR-mediated inhibition of Ca^{2+} absorption in in vitro and ex vivo. (**A**) Effect of CaSR activation on Ca^{2+}-induced currents (I_{Ca}) in TRPV6 expressing oocytes in the presence and absence of cinacalcet and/or U73122, a phospholipase C (PLC) inhibitor (n = 6 each). Mean I_{Ca} values obtained from TRPV6- and CaSR-expressing oocytes were normalized to vehicle I_{Ca} values from TRPV6-expressing oocytes ± SEM; asterisks indicate a statistically significant difference between the conditions (multiple-comparisons Kruskal-Wallis test; *$P < 0.05$; **$P < 0.01$). (**B**) Effect of cinacalcet and/or U73122 on the plasma membrane expression of TRPV6 and CaSR in oocytes determined by immunoblot. As a loading control, β-actin was blotted (bottom). (**C**) Quantification of surface TRPV6 expression, normalized to total TRPV6 (n = 3 each). (**D**) Effect of basolateral cinacalcet (10 μM) and vehicle (DMSO) or PLC inhibitor U73122 (10 μM) on mouse proximal colon (n = 6 each). Raw values are presented; asterisks indicate a statistical difference between the conditions (Student's paired t tests; *$P < 0.05$).

Acute regulation of epithelial membrane channels can be accomplished by alterations in channel function or membrane expression. Membrane expression of TRPV5, a close family member of TRPV6, is altered in the DCT/CNT, thereby regulating channel activity (54, 55). Therefore, we assessed whether CaSR-mediated TRPV6 regulation was the result of alterations in membrane expression. This was not the case. In *Xenopus* oocytes expressing TRPV6 and the CaSR, cinacalcet had no effect on membrane expression of TRPV6. Unlike the changes in intestinal expression of *Trpv6* mediated by chronic cinacalcet administration, acute changes in TRPV6-mediated Ca^{2+} flux are likely due to a CaSR-mediated regulation of TRPV6 activity, rather than expression.

Activation of the CaSR stimulates a network of cell-signaling pathways. In colonocytes, CaSR activation alters fluid absorption via PLC (32, 34). Consistent with this, PLC inhibition prevented decreased Ca^{2+} flux through TRPV6 in response to activation of the CaSR both in vitro and ex vivo. PLC is a membrane-bound phospholipase that catalyzes phosphatidylinositol 4,5-bisphosphate (PIP_2) into diacylglycerol and inositol triphosphate (IP3), and IP3 increases intracellular Ca^{2+} (56), a signaling pathway used by the CaSR in the parathyroid (34). TRPV6 activity is upregulated by PIP_2 and downregulated by intracellular Ca^{2+} (57). Extracellular Ca^{2+} inhibits TRPV6 via PIP_2 hydrolysis in whole-cell patch clamp experiments and everted duodenal gut sac $^{45}Ca^{2+}$ transport assays (46, 47). Furthermore, increased intracellular Ca^{2+}, another consequence of PLC activation, directly inhibits TRPV6, providing another molecular explanation for how CaSR activation could inhibit TRPV6 (57, 58). Regardless of the exact downstream mechanism, our data provide evidence of intestinal CaSR-mediated PLC regulation of TRPV6 function.

The currently accepted model of intestinal Ca^{2+} absorption is that the duodenum, cecum, and proximal colon are capable of both transcellular and paracellular Ca^{2+} absorption while the jejunum and ileum contribute only paracellular Ca^{2+} absorption and/or secretion (23, 59, 60). There has been greater emphasis on the duodenum as a site of Ca^{2+} absorption and regulation recently (61); however, a significant role for the proximal large bowel in mediating intestinal Ca^{2+} absorption in humans and rodents has been appreciated

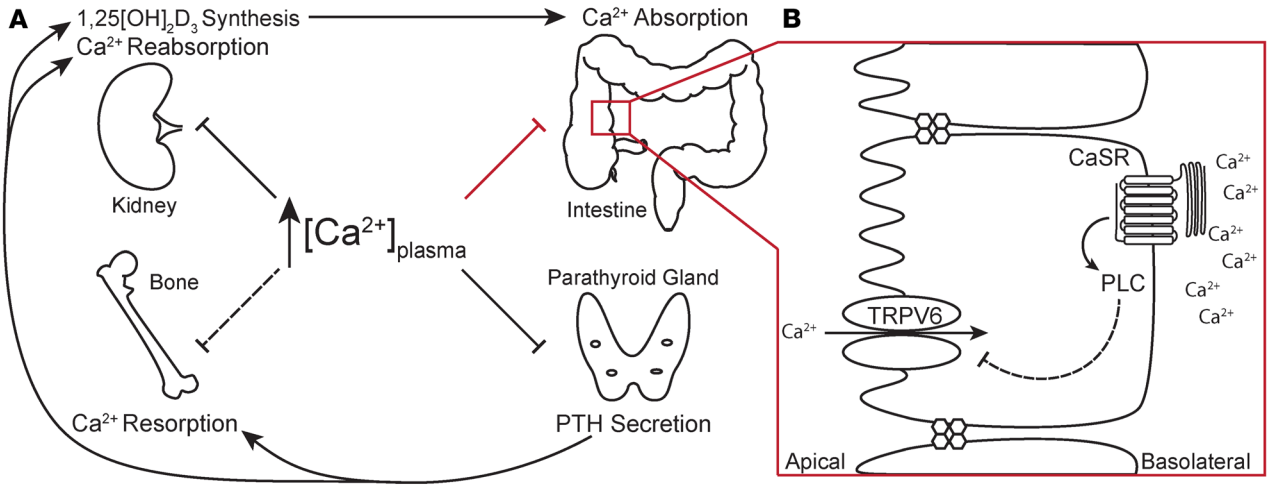

Figure 7. Proposed model of CaSR-mediated inhibition of Ca^{2+} absorption. (**A**) Increased plasma Ca^{2+} is sensed by the CaSR expressed in kidneys, bone, intestine, and parathyroid glands. In response, the kidneys decrease Ca^{2+} reabsorption, there is decreased bone resorption, and parathyroid hormone (PTH) secretion is decreased. We show herein that intestinal Ca^{2+} absorption is inhibited. In concert, this reduces plasma Ca^{2+}. Importantly, PTH acts to increase plasma Ca^{2+} by increasing bone Ca^{2+} resorption, renal tubular reabsorption, and indirectly by increasing intestinal Ca^{2+} absorption by increasing 1,25-$[OH]_2$ D_3 synthesis in the kidneys. (**B**) High plasma Ca^{2+} is detected by the intestinal epithelial basolateral CaSR, which inhibits TRPV6-mediated transcellular Ca^{2+} transport via PLC.

for decades (62–65). In addition, multiple studies support the presence of 1,25-$[OH]_2$ D_3–mediated regulation of transcellular Ca^{2+} absorption from the proximal large bowel (38, 39, 64–66). Thus, the contribution of this segment to overall Ca^{2+} homeostasis should be considered. Our work provides further evidence the proximal colon plays a regulatory role in Ca^{2+} homeostasis. We have identified a potentially novel regulatory mechanism present in the proximal large bowel, which includes a Ca^{2+}-sensing mechanism that detects altered extracellular Ca^{2+} and amends Ca^{2+} absorption to restore plasma Ca^{2+}. We hypothesize that the luminal Ca^{2+} that is not absorbed from the duodenum and distal small bowel is likely subjected to fine regulation by the proximal large bowel, which senses the body's extracellular Ca^{2+} and fine-tunes Ca^{2+} absorption and consequently fecal excretion to maintain plasma Ca^{2+} within the physiological range. Interestingly, a similar Ca^{2+}-handling mechanism is observed in renal tubules. After significant paracellular reabsorption from the proximal tubule and the TAL, urinary Ca^{2+} excretion is fine-tuned in the more distal DCT/CNT segments by a transcellular pathway analogous to the one observed in the proximal large bowel (54, 67). Our results reveal that these pathways share a similar regulatory mechanism, a direct Ca^{2+}-sensing mechanism that affects Ca^{2+} transport. Further, the DCT/CNT and the large bowel have both been estimated to contribute 10% of Ca^{2+} reabsorption in their respective organs (61, 68). Together, our findings highlight a substantial Ca^{2+} regulatory role in the proximal large bowel and challenge the prevailing contention that this segment is not important for Ca^{2+} homeostasis.

The administration of cinacalcet to dialysis patients often causes hypocalcemia (69–71). This has been attributed to hungry bone syndrome, via rapid lowering of plasma PTH. Our work provides an alternative explanation for this observation. Cinacalcet administration would not only attenuate release of PTH from the parathyroid but also inhibit Ca^{2+} absorption from the intestine, thereby lowering plasma Ca^{2+} levels.

In conclusion, we demonstrate a Ca^{2+}-sensing mechanism present in the proximal large bowel that regulates Ca^{2+} absorption through a transcellular pathway, both acutely and chronically. The transcellular pathway mediating this effect relies on apical Ca^{2+} influx through TRPV6 because this effect was absent in $TRPV6^{D541A/D541A}$-mutant mice. The CaSR appears to be the sensor of extracellular Ca^{2+} because the pathway can be reconstituted in vitro by coexpressing the CaSR and TRPV6 in *Xenopus* oocytes. The cellular mechanism contributing to acute CaSR modulation of TRPV6 function involves PLC activation, which ultimately results in TRPV6 inactivation. This might be via a decrease in PIP_2 levels or an increase in intracellular Ca^{2+}. These studies contribute to our understanding of Ca^{2+} homeostasis, providing evidence that the proximal large bowel can sense extracellular Ca^{2+} and adjust intestinal Ca^{2+} absorption to maintain plasma Ca^{2+} levels.

Methods

Mice. Wild-type FVB/N mice (Jackson Laboratory) and Trpv6$^{D541A/D541A}$-knockin mice (43) were housed in virus-free conditions and maintained on a 12-hour light/12-hour dark cycle. The TRPV6$^{D541A/D541A}$ mice were backcrossed to FVB/N for more than 5 generations. Standard pelleted chow (PicoLab Rodent Diet 5053: 21% wt/wt protein, 5.0% wt/wt fat, 0.81% wt/wt Ca^{2+}, and 2.2 IU/g vitamin D_3) and drinking water were available ad libitum. The experiments with respect to chronic altered Ca^{2+}-containing diets (21 days) and treatment with 1,25-$[OH]_2$ D_3 (5 days) and cinacalcet (Santa Cruz Biotechnology) (5 days) were performed and described previously (15).

Real-time quantitative PCR. Following euthanasia, the duodenum, cecum, and proximal colon were collected as previously described (25). Total RNA was isolated using TRIzol Reagent and reverse-transcribed into cDNA using Random Primers and SuperScript II reverse transcriptase (all from Invitrogen). Primers and probes (Integrated DNA Technologies) designed for TRPV6 (*Trpv6*), CABP9K (*S100g*), NCX1 (*Slc8a1*), PMCA1b (*Atp2b1*), and CaSR (*CaSR*) were used to quantify expression levels with an ABI Prism 7900 HT Sequence Detection System (Applied Biosystems).

Ussing chamber experiments. $^{45}Ca^{2+}$ flux across the duodenum, cecum, and proximal colon of 8- to 12-week-old FVB/N, Trpv6$^{WT/WT}$, and Trpv6$^{D541A/D541A}$ mice was performed essentially as previously (72). Following euthanasia, whole-wall duodenal, cecal, and proximal colonic intestinal sections of FVB/N, Trpv6$^{WT/WT}$, and Trpv6$^{D541A/D541A}$ mice were dissected, linearized, and transversely cut into 3-mm segments. NB: Whole-wall intestinal sections used as sections with seromuscular layer stripped did not behave differently (72). These segments were mounted in an Ussing chamber (EM-CYS-4 system with P2400 chambers and P2407B sliders, Physiologic Instruments) and incubated with 4 ml Ringer's solution consisting of 115 mM NaCl, 2.5 mM K_2HPO_4, 40 mM KH_2PO_4, 1.2 mM $MgCl_2$, 1.2 mM $CaCl_2$, and 25 mM $NaHCO_3$, bubbled with 5% vol/vol CO_2, 95% vol/vol O_2 at 37°C on both sides. Apical and basolateral solutions contained 10 mM mannitol, 10 mM glucose, and 2 μM indomethacin (bilateral, MilliporeSigma). The basolateral solution also contained 0.1 μM tetrodotoxin (Alomone Labs). The transepithelial potential difference was clamped to 0 mV by a VCC MC6 Multichannel Voltage/Current Clamp (Physiologic Instruments) and the resulting short-circuit current recorded with Acquire & Analyze software (Physiologic Instruments) through Ag-AgCl electrodes and 3 M KCl agarose bridges. The TER was calculated using Ohm's law, following the measurement of the current generated in response to 2-mV pulses lasting 2.5 seconds, applied every 100 seconds.

Unidirectional Ca^{2+} fluxes (i.e., apical to basolateral or basolateral to apical) were measured using the protocol shown in Figure 2. At time 0, either the apical or basolateral solution was exchanged for a fresh solution of the same composition spiked with 5 μCi/ml $^{45}Ca^{2+}$. Three samples (50 μl each) were taken from both chambers at 15-minute intervals throughout each experimental condition (condition A: sample taken at 20, 35, and 50 minutes; condition B: samples taken at 75, 90, and 105 minutes). After the third sample was collected under condition A, the buffers were immediately changed and/or treatments applied (i.e., 10 μM cinacalcet hydrochloride [cinacalcet] in ethanol or 10 μM U73122 in DMSO), and the tissue was incubated for another 20 minutes before sampling for condition B. Radioactivity was measured with an LS6500 Multi-Purpose Scintillation Counter (Beckman Coulter), and unidirectional Ca^{2+} fluxes in opposite directions were paired to calculate net Ca^{2+} flux (net apical-to-basolateral flux). All Ussing chamber fluxes were normalized to surface area (cm^2) before analysis. A total of 4 pairs were made per animal, and only pairs with less than 25% difference in TER were considered (changes in TER are shown in Supplemental Table 1).

Xenopus oocyte expression and 2-electrode voltage clamp. The preparation of *Xenopus* oocytes and the 2-electrode voltage clamp experiments were performed as previously described (73). Capped RNA of human TRPV6 (accession number NM_018646, generated using in vitro transcription with mMESSAGE mMACHINE kit by Ambion) and human CaSR cDNA (Origene; catalog RC211229) were injected into *Xenopus* oocytes. Two days after injection, whole-cell Ca^{2+} currents of oocytes were recorded at room temperature in a standard extracellular solution containing 100 mM NaCl, 2 mM KCl, 1 mM $MgCl_2$, and 10 mM HEPES (pH 7.5) with 5 mM Ca^{2+}. Baseline current was determined by using the solution above but without 5 mM Ca^{2+}. The 2 electrodes (capillary pipettes; Warner Instruments) impaling an oocyte were filled with 3 M KCl to form a tip resistance of 0.3–2 MΩ. A Geneclamp 500B amplifier and Digidata 1322A AD/DA converter (Molecular Devices) were used to obtain the currents. pClamp 9 software (Axon Instruments) was used for data acquisition and analysis. Currents and voltages were digitally recorded at 200 ms/sample and filtered at 2 kHz through a Bessel filter. Sigma Plot 14 (Systat Software) was used for plotting data.

Oocytes' surface protein expression was determined with a biotinylation assay as previously described (73). In short, the oocytes were incubated with 0.5 mg/ml sulfo-NHS-SS-Biotin (Pierce) for 30 minutes at room temperature, and nonreacted biotin was quenched with 1 M NH_4Cl. After a wash, oocytes were harvested in ice-cold CellLytic M lysis buffer (MilliporeSigma) with a 1 times proteinase inhibitor mixture (Thermo Fisher Scientific). The surface proteins were absorbed by 100 µl streptavidin (Pierce) at 4°C overnight and subjected to SDS-PAGE. Mouse primary anti-CaSR monoclonal antibody (1:2000, Gentex, catalog GTX19347), in-house–generated anti-TRPV6 polyclonal antibody (1:1000) (74), mouse primary anti–β-actin monoclonal antibody (1:1000, Santa Cruz Biotechnology, catalog sc-47778), and horseradish peroxidase–coupled secondary antibody (1:5000, Santa Cruz Biotechnology, catalog sc-2005) were used for immunoblotting. The immunoblots were quantified using ImageJ software (NIH).

Statistics. Data are presented as mean ± SEM, and all data reported are based on measurements made on more than 6 animals (minimum 3 males and 3 females). A Shapiro-Wilk test was performed to assess for normal distribution. One-way ANOVA, Brown-Forsythe test, Kruskal-Wallis test, and Student's unpaired or paired 2-tailed *t* tests (GraphPad) were carried out to determine statistical significance as appropriate, and *P* values less than 0.05 were considered statistically significant.

Study approval. All animal experiments were approved by the Animal Care and Use Committee for Health Science of the University of Alberta (protocol 213 for mouse and 234 for frog) and followed the *Guide for the Care and Use of Laboratory Animals* (National Academies Press, 2011).

Author contributions

JJL, HD, and RTA conceived of and designed the research study. JJL, XL, DO, HD, and RTA performed experiments. PW and VF provided $TRPV6^{D451A}$ mice. JJL, XL, and RTA analyzed data. JJL, XL, MRB, HD, and RTA interpreted results of experiments. JJL and RTA prepared figures and drafted the manuscript; JJL, XL, DO, MRB, PW, VF, XZC, HD, and RTA edited, revised, and approved the final version of the manuscript.

Acknowledgments

This work was funded by grants from the Women and Children's Health Research Institute, which is supported by the Stollery Children's Hospital Foundation, and the National Sciences and Engineering Research Council (grant 05842) to RTA, who is the Canada Research Chair in Renal Epithelial Transport Physiology. HD is supported by Fabrikant Vilhelm Pedersen og Hustrus Mindelegat, the Novo Nordisk Foundation, the Beckett Foundation, the Lundbeck Foundation, and the Independent Research Fund Denmark. PW and VF are supported by Deutsche Forschungsgemeinschaft by Sonderforschungsbereich 894. MRB is supported by a Vanier Canada Graduate Scholarship.

Address correspondence to: R. Todd Alexander, Department of Pediatrics, 4-585 Edmonton Clinic Health Academy, 11405 87th Avenue, University of Alberta, Edmonton, Alberta, T6G 2R7, Canada. Phone: 780.248.1493; Email: todd2@ualberta.ca.

1. Blau JE, Collins MT. The PTH-Vitamin D-FGF23 axis. *Rev Endocr Metab Disord*. 2015;16(2):165–174.
2. Fleet JC. The role of vitamin D in the endocrinology controlling calcium homeostasis. *Mol Cell Endocrinol*. 2017;453:36–45.
3. Khundmiri SJ, Murray RD, Lederer E. PTH and vitamin D. *Compr Physiol*. 2016;6(2):561–601.
4. Rodríguez-Ortiz ME, Rodríguez M. FGF23 as a calciotropic hormone. *F1000Res*. 2015;4:F1000.
5. Toka HR, Pollak MR, Houillier P. Calcium sensing in the renal tubule. *Physiology (Bethesda)*. 2015;30(4):317–326.
6. Goltzman D, Hendy GN. The calcium-sensing receptor in bone — mechanistic and therapeutic insights. *Nat Rev Endocrinol*. 2015;11(5):298–307.
7. Brown EM. Role of the calcium-sensing receptor in extracellular calcium homeostasis. *Best Pract Res Clin Endocrinol Metab*. 2013;27(3):333–343.
8. Fleet JC, Eksir F, Hance KW, Wood RJ. Vitamin D-inducible calcium transport and gene expression in three Caco-2 cell lines. *Am J Physiol Gastrointest Liver Physiol*. 2002;283(3):G618–G625.
9. Song Y, et al. Calcium transporter 1 and epithelial calcium channel messenger ribonucleic acid are differentially regulated by 1,25 dihydroxyvitamin D3 in the intestine and kidney of mice. *Endocrinology*. 2003;144(9):3885–3894.
10. Cui M, Zhao Y, Hance KW, Shao A, Wood RJ, Fleet JC. Effects of MAPK signaling on 1,25-dihydroxyvitamin D-mediated CYP24 gene expression in the enterocyte-like cell line, Caco-2. *J Cell Physiol*. 2009;219(1):132–142.
11. Walters JR, et al. Calcium channel TRPV6 expression in human duodenum: different relationships to the vitamin D system and aging in men and women. *J Bone Miner Res*. 2006;21(11):1770–1777.
12. Posillico JT, Srikanta S, Eisenbarth G, Quaranta V, Kajiji S, Brown EM. Binding of monoclonal antibody (4F2) to its cell surface antigen on dispersed adenomatous parathyroid cells raises cytosolic calcium and inhibits parathyroid hormone secretion.

J Clin Endocrinol Metab. 1987;64(1):43–50.
13. Brown AJ, Zhong M, Ritter C, Brown EM, Slatopolsky E. Loss of calcium responsiveness in cultured bovine parathyroid cells is associated with decreased calcium receptor expression. *Biochem Biophys Res Commun*. 1995;212(3):861–867.
14. Ho C, et al. A mouse model of human familial hypocalciuric hypercalcemia and neonatal severe hyperparathyroidism. *Nat Genet*. 1995;11(4):389–394.
15. Dimke H, Desai P, Borovac J, Lau A, Pan W, Alexander RT. Activation of the Ca(2+)-sensing receptor increases renal claudin-14 expression and urinary Ca(2+) excretion. *Am J Physiol Renal Physiol*. 2013;304(6):F761–F769.
16. Gong Y, Hou J. Claudin-14 underlies Ca^{++}-sensing receptor-mediated Ca^{++} metabolism via NFAT-microRNA-based mechanisms. *J Am Soc Nephrol*. 2014;25(4):745–760.
17. Gong Y, et al. Claudin-14 regulates renal Ca^{++} transport in response to CaSR signalling via a novel microRNA pathway. *EMBO J*. 2012;31(8):1999–2012.
18. Loupy A, et al. PTH-independent regulation of blood calcium concentration by the calcium-sensing receptor. *J Clin Invest*. 2012;122(9):3355–3367.
19. Sato T, et al. Parathyroid hormone controls paracellular Ca. *Proc Natl Acad Sci U S A*. 2017;114(16):E3344–E3353.
20. Hoover RS, Tomilin V, Hanson L, Pochynyuk O, Ko B. PTH modulation of NCC activity regulates TRPV5 Ca^{2+} reabsorption. *Am J Physiol Renal Physiol*. 2016;310(2):F144–F151.
21. Boros S, Bindels RJ, Hoenderop JG. Active Ca(2+) reabsorption in the connecting tubule. *Pflugers Arch*. 2009;458(1):99–109.
22. de Groot T, et al. Parathyroid hormone activates TRPV5 via PKA-dependent phosphorylation. *J Am Soc Nephrol*. 2009;20(8):1693–1704.
23. Hoenderop JG, Nilius B, Bindels RJ. Calcium absorption across epithelia. *Physiol Rev*. 2005;85(1):373–422.
24. Christakos S, Dhawan P, Porta A, Mady LJ, Seth T. Vitamin D and intestinal calcium absorption. *Mol Cell Endocrinol*. 2011;347(1–2):25–29.
25. Pan W, et al. The epithelial sodium/proton exchanger, NHE3, is necessary for renal and intestinal calcium (re)absorption. *Am J Physiol Renal Physiol*. 2012;302(8):F943–F956.
26. Alexander RT, et al. Klotho prevents renal calcium loss. *J Am Soc Nephrol*. 2009;20(11):2371–2379.
27. Wongdee K, Charoenphandhu N. Vitamin D-enhanced duodenal calcium transport. *Vitam Horm*. 2015;98:407–440.
28. Benn BS, et al. Active intestinal calcium transport in the absence of transient receptor potential vanilloid type 6 and calbindin-D9k. *Endocrinology*. 2008;149(6):3196–3205.
29. Xue Y, Fleet JC. Intestinal vitamin D receptor is required for normal calcium and bone metabolism in mice. *Gastroenterology*. 2009;136(4):1317–e2.
30. Gama L, Baxendale-Cox LM, Breitwieser GE. Ca^{2+}-sensing receptors in intestinal epithelium. *Am J Physiol*. 1997;273(4 pt 1):C1168–C1175.
31. Chattopadhyay N, et al. Identification and localization of extracellular Ca(2+)-sensing receptor in rat intestine. *Am J Physiol*. 1998;274(1 Pt 1):G122–G130.
32. Cheng SX, Okuda M, Hall AE, Geibel JP, Hebert SC. Expression of calcium-sensing receptor in rat colonic epithelium: evidence for modulation of fluid secretion. *Am J Physiol Gastrointest Liver Physiol*. 2002;283(1):G240–G250.
33. Tang L, Cheng CY, Sun X, Pedicone AJ, Mohamadzadeh M, Cheng SX. The extracellular calcium-sensing receptor in the intestine: evidence for regulation of colonic absorption, secretion, motility, and immunity. *Front Physiol*. 2016;7:245.
34. Geibel J, et al. Calcium-sensing receptor abrogates secretagogue- induced increases in intestinal net fluid secretion by enhancing cyclic nucleotide destruction. *Proc Natl Acad Sci U S A*. 2006;103(25):9390–9397.
35. Cui M, Li Q, Johnson R, Fleet JC. Villin promoter-mediated transgenic expression of transient receptor potential cation channel, subfamily V, member 6 (TRPV6) increases intestinal calcium absorption in wild-type and vitamin D receptor knockout mice. *J Bone Miner Res*. 2012;27(10):2097–2107.
36. Lee GS, Jung EM, Choi KC, Oh GT, Jeung EB. Compensatory induction of the TRPV6 channel in a calbindin-D9k knockout mouse: Its regulation by 1,25-hydroxyvitamin D3. *J Cell Biochem*. 2009;108(5):1175–1183.
37. van Abel M, Hoenderop JG, van der Kemp AW, van Leeuwen JP, Bindels RJ. Regulation of the epithelial Ca^{2+} channels in small intestine as studied by quantitative mRNA detection. *Am J Physiol Gastrointest Liver Physiol*. 2003;285(1):G78–G85.
38. Favus MJ, Kathpalia SC, Coe FL, Mond AE. Effects of diet calcium and 1,25-dihydroxyvitamin D3 on colon calcium active transport. *Am J Physiol*. 1980;238(2):G75–G78.
39. Favus MJ, Kathpalia SC, Coe FL. Kinetic characteristics of calcium absorption and secretion by rat colon. *Am J Physiol*. 1981;240(5):G350–G354.
40. Rutten MJ, et al. Identification of a functional Ca^{2+}-sensing receptor in normal human gastric mucous epithelial cells. *Am J Physiol*. 1999;277(3):G662–G670.
41. Sheinin Y, Kállay E, Wrba F, Kriwanek S, Peterlik M, Cross HS. Immunocytochemical localization of the extracellular calcium-sensing receptor in normal and malignant human large intestinal mucosa. *J Histochem Cytochem*. 2000;48(5):595–602.
42. Cheng SX, et al. Epithelial CaSR deficiency alters intestinal integrity and promotes proinflammatory immune responses. *FEBS Lett*. 2014;588(22):4158–4166.
43. Weissgerber P, et al. Male fertility depends on Ca^{2+} absorption by TRPV6 in epididymal epithelia. *Sci Signal*. 2011;4(171):ra27.
44. Peng JB, et al. Molecular cloning and characterization of a channel-like transporter mediating intestinal calcium absorption. *J Biol Chem*. 1999;274(32):22739–22746.
45. Nilius B, Owsianik G, Voets T. Transient receptor potential channels meet phosphoinositides. *EMBO J*. 2008;27(21):2809–2816.
46. Thyagarajan B, Benn BS, Christakos S, Rohacs T. Phospholipase C-mediated regulation of transient receptor potential vanilloid 6 channels: implications in active intestinal Ca^{2+} transport. *Mol Pharmacol*. 2009;75(3):608–616.
47. Thyagarajan B, Lukacs V, Rohacs T. Hydrolysis of phosphatidylinositol 4,5-bisphosphate mediates calcium-induced inactivation of TRPV6 channels. *J Biol Chem*. 2008;283(22):14980–14987.
48. Vachel L, Norez C, Jayle C, Becq F, Vandebrouck C. The low PLC-δ1 expression in cystic fibrosis bronchial epithelial cells induces upregulation of TRPV6 channel activity. *Cell Calcium*. 2015;57(1):38–48.
49. Zakharian E, Cao C, Rohacs T. Intracellular ATP supports TRPV6 activity via lipid kinases and the generation of PtdIns(4,5)

P_2. *FASEB J*. 2011;25(11):3915–3928.
50. Van Cromphaut SJ, et al. Duodenal calcium absorption in vitamin D receptor-knockout mice: functional and molecular aspects. *Proc Natl Acad Sci U S A*. 2001;98(23):13324–13329.
51. Weber K, Erben RG, Rump A, Adamski J. Gene structure and regulation of the murine epithelial calcium channels ECaC1 and 2. *Biochem Biophys Res Commun*. 2001;289(5):1287–1294.
52. Woudenberg-Vrenken TE, et al. Functional TRPV6 channels are crucial for transepithelial Ca^{2+} absorption. *Am J Physiol Gastrointest Liver Physiol*. 2012;303(7):G879–G885.
53. Plain A, et al. Corticomedullary difference in the effects of dietary Ca^{2+} on tight junction properties in thick ascending limbs of Henle's loop. *Pflugers Arch*. 2016;468(2):293–303.
54. Topala CN, Schoeber JP, Searchfield LE, Riccardi D, Hoenderop JG, Bindels RJ. Activation of the Ca^{2+}-sensing receptor stimulates the activity of the epithelial Ca^{2+} channel TRPV5. *Cell Calcium*. 2009;45(4):331–339.
55. Hoenderop JG, et al. Calcitriol controls the epithelial calcium channel in kidney. *J Am Soc Nephrol*. 2001;12(7):1342–1349.
56. Conigrave AD, Ward DT. Calcium-sensing receptor (CaSR): pharmacological properties and signaling pathways. *Best Pract Res Clin Endocrinol Metab*. 2013;27(3):315–331.
57. Bödding M, Flockerzi V. Ca^{2+} dependence of the Ca^{2+}-selective TRPV6 channel. *J Biol Chem*. 2004;279(35):36546–36552.
58. Hoenderop JG, et al. Function and expression of the epithelial Ca(2+) channel family: comparison of mammalian ECaC1 and 2. *J Physiol (Lond)*. 2001;537(Pt 3):747–761.
59. Favus MJ. Factors that influence absorption and secretion of calcium in the small intestine and colon. *Am J Physiol*. 1985;248(2 pt 1):G147–G157.
60. Bronner F, Pansu D, Stein WD. An analysis of intestinal calcium transport across the rat intestine. *Am J Physiol*. 1986;250(5 pt 1):G561–G569.
61. Bronner F, Pansu D. Nutritional aspects of calcium absorption. *J Nutr*. 1999;129(1):9–12.
62. Hylander E, Ladefoged K, Jarnum S. Calcium absorption after intestinal resection. The importance of a preserved colon. *Scand J Gastroenterol*. 1990;25(7):705–710.
63. Hylander E, Ladefoged K, Jarnum S. The importance of the colon in calcium absorption following small-intestinal resection. *Scand J Gastroenterol*. 1980;15(1):55–60.
64. Karbach U, Feldmeier H. The cecum is the site with the highest calcium absorption in rat intestine. *Dig Dis Sci*. 1993;38(10):1815–1824.
65. Petith MM, Schedl HP. Intestinal adaptation to dietary calcium restriction: in vivo cecal and colonic calcium transport in the rat. *Gastroenterology*. 1976;71(6):1039–1042.
66. Harrison HC, Harrison HE. Calcium transport by rat colon in vitro. *Am J Physiol*. 1969;217(1):121–125.
67. Huang C, et al. Interaction of the Ca^{2+}-sensing receptor with the inwardly rectifying potassium channels Kir4.1 and Kir4.2 results in inhibition of channel function. *Am J Physiol Renal Physiol*. 2007;292(3):F1073–F1081.
68. Moor MB, Bonny O. Ways of calcium reabsorption in the kidney. *Am J Physiol Renal Physiol*. 2016;310(11):F1337–F1350.
69. Block GA, et al. Cinacalcet for secondary hyperparathyroidism in patients receiving hemodialysis. *N Engl J Med*. 2004;350(15):1516–1525.
70. Brunelli SM, Dluzniewski PJ, Cooper K, Do TP, Sibbel S, Bradbury BD. Management of serum calcium reductions among patients on hemodialysis following cinacalcet initiation. *Pharmacoepidemiol Drug Saf*. 2015;24(10):1058–1067.
71. Floege J, Tsirtsonis K, Iles J, Drueke TB, Chertow GM, Parfrey P. Incidence, predictors and therapeutic consequences of hypocalcemia in patients treated with cinacalcet in the EVOLVE trial. *Kidney Int*. 2018;93(6):1475–1482.
72. Rievaj J, Pan W, Cordat E, Alexander RT. The Na^+/H^+ exchanger isoform 3 is required for active paracellular and transcellular Ca^{2+} transport across murine cecum. *Am J Physiol Gastrointest Liver Physiol*. 2013;305(4):G303–G313.
73. Zheng W, et al. Hydrophobic pore gates regulate ion permeation in polycystic kidney disease 2 and 2L1 channels. *Nat Commun*. 2018;9(1):2302.
74. Fecher-Trost C, et al. The in vivo TRPV6 protein starts at a non-AUG triplet, decoded as methionine, upstream of canonical initiation at AUG. *J Biol Chem*. 2013;288(23):16629–16644.